ACS APPLIED MATERIALS & INTERFACES

www.acsami.org

Research Article

Synthetic Heparan Sulfate Hydrogels Regulate Neurotrophic Factor Signaling and Neuronal Network Activity

Charles-Francois V. Latchoumane,[¶] Pradeep Chopra,[¶] Lifeng Sun, Aws Ahmed, Francesco Palmieri, Hsueh-Fu Wu, Rebecca Guerreso, Kristen Thorne, Nadja Zeltner, Geert-Jan Boons,* and Lohitash Karumbaiah*

Cite This: *ACS Appl. Mater. Interfaces* 2022, 14, 28476–28488

Read Online

ACCESS | Metrics & More | Article Recommendations | Supporting Information

ABSTRACT: Three-dimensional (3D) synthetic heparan sulfate (HS) constructs possess promising attributes for neural tissue engineering applications. However, their sulfation-dependent ability to facilitate molecular recognition and cell signaling has not yet been investigated. We hypothesized that fully sulfated synthetic HS constructs (bearing compound **1**) that are functionalized with neural adhesion peptides will enhance fibroblast growth factor-2 (FGF2) binding and complexation with FGF receptor-1 (FGFR1) to promote the proliferation and neuronal differentiation of human neural stem cells (hNSCs) when compared to constructs with unsulfated controls (bearing compound **2**). We tested this hypothesis *in vitro* using 2D and 3D substrates consisting of different combinations of HS tetrasaccharides (compounds **3** and **4**) and an engineered integrin-binding chimeric peptide (CP), which were assembled using strain-promoted alkyne-azide cycloaddition (SPAAC) chemistry. Results indicated that the adhesion of hNSCs increased significantly when cultured on 2D glass substrates functionalized with chimeric peptide. hNSCs encapsulated in **1**-CP hydrogels and cultured in media containing the mitogen FGF2 exhibited significantly higher neuronal differentiation when compared to hNSCs in **2**-CP hydrogels. These observations were corroborated by Western blot analysis, which indicated the enhanced binding and retention of both FGF2 and FGFR1 by **1** as well as downstream phosphorylation of extracellular signal-regulated kinases (ERK1/2) and enhanced proliferation of hNSCs. Lastly, calcium activity imaging revealed that both **1** and **2** hydrogels supported the neuronal growth and activity of pre-differentiated human prefrontal cortex neurons. Collectively, these results demonstrate that synthetic HS hydrogels can be tailored to regulate growth factor signaling and neuronal fate and activity.

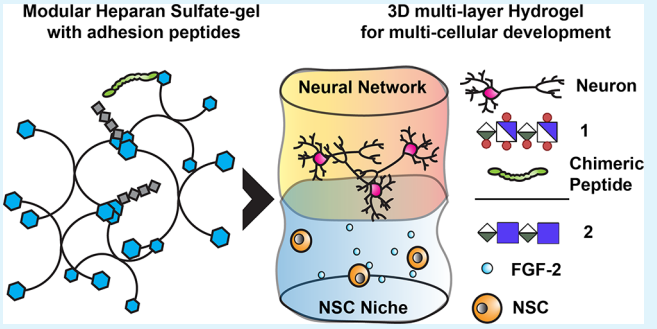

KEYWORDS: *synthetic heparan sulfate hydrogel, ERK, FGF2, neural stem cells, click chemistry*

INTRODUCTION

Heparan sulfates (HS) are linear anionic polysaccharides consisting of alternating glucosamine (GlcN) and glucuronic (GlcA) or iduronic acid (IdoA) residues that are linked to a core protein to form heparan sulfate proteoglycans (HSPGs).[1] HSPGs in the adult brain are distinctly localized in the basement membrane and the synaptic cleft. Diversely sulfated epitopes on HS chains regulate trophic factor binding and cellular signaling to promote angiogenesis[2] as well as neurogenesis and plasticity.[3,4] HS interactions with the cell regulatory mitogen, fibroblast growth factor (FGF), and family of cognate FGF receptors (FGFRs) have been the subject of much investigation.[5] However, most of these interactions have been elucidated using specific binding affinity assays, which are not designed to provide biological information regarding protein complexation and downstream signaling using hydrogel-based cellular bioassays.[6]

In invertebrates, HS has been reported to direct neural stem cell (NSC) migration and neuronal differentiation.[4,7,8] FGF2 is a major regulator of NSC proliferation and neurogenesis, which signals mainly through FGFR1 present on NSCs and neurons in the developing and adult central nervous system.[9] In addition to promoting NSC proliferation, FGF2 is also important for neuronal differentiation,[10] axonal branching,[11] and plasticity. Axonal growth and plasticity in the brain are also regulated by extracellular matrix proteins such as laminin, which regulates neuronal cell adhesion *via* the presentation of integrin binding sites such as RGDS and IKVAV.[12,13] Previous studies have demonstrated that a hybrid chimeric peptide containing these epitopes[13,14] promoted the adhesion and

Received: January 27, 2022
Accepted: June 6, 2022
Published: June 16, 2022

differentiation of neurons. Other reports have also demonstrated that specific motifs in laminin,[15] neural cell adhesion molecules,[16] N-cadherin,[16,17] and L1[16] proteins can synergistically promote FGF2- and FGFR1-mediated neuritogenesis and proliferation. However, the integration of these cell instructive peptide motifs with the high-affinity FGF2-regulating attributes of sulfated HS tetrasaccharides in a 3D biomaterial that is designed to support cell adhesion, NSC proliferation, neuronal differentiation, and neuronal activity has so far not been explored.

Previously, we demonstrated that a hydrogel modified by an HS-disaccharide supports the maintenance of hNSCs *in vitro*.[18] Here, we hypothesized that 3D hydrogel constructs consisting of fully sulfated HS tetrasaccharides and neuronal cell adhesion-promoting peptides will enhance FGF2-FGFR1 complexation, leading to enhanced proliferation and neuronal differentiation of hydrogel-encapsulated hNSCs when compared to unsulfated controls. We describe the design of a hydrogel construct consisting of a well-defined, fully sulfated HS tetrasaccharide and a cell adhesion-promoting peptide derived from laminin that can potentiate the activity of FGF2 to promote NSC proliferation, neuronal differentiation, and activity of differentiated neurons. The HS tetrasaccharide was selected because it is the smallest active unit that can bind to FGF2 and induce cell signaling by providing transient stabilization of the FGF2-FGFR1 complex.[19,20] First, we used 2D functionalized glass slides to evaluate chimeric peptide concentration-dependent neuronal adhesion and assessed sulfation-dependent enhanced binding of FGF2 and FGFR1 in a microarray format. Next, we examined hNSC proliferation and differentiation in sulfated HS tetrasaccharide (**1**) and unsulfated (**2**) control hydrogels using Western blotting and immunocytochemistry. Finally, we used calcium imaging to investigate the potential of differentially sulfated HS hydrogels to support neuronal activity.

MATERIALS AND METHODS

Chemical Synthesis. *Peptide Synthesis.* Azide-functionalized peptides, RGDS, YIGSR, IKVAV, and chimeric peptide were synthesized on Wang resin or rink amide resin (Novabiochem, San Diego, CA, 0.1 mmol) by established protocols on a CEM Liberty Automated Microwave Peptide Synthesizer using standard Fmoc-protected amino acids. The peptides were purified by high-pressure liquid chromatography (HPLC) and characterized using MS (MALDI-ToF, Applied Biosystems 5800).

General Procedure for Chemical Glycosylation. The solution of glycosyl acceptor (1.0 equiv), donor (1.2 equiv), and activated molecular sieves (4 Å) in CH_2Cl_2 (0.2 M) was placed under an atmosphere of argon, and the resulting suspension was stirred at room temperature for 0.5 h. The mixture was cooled to −20 °C, trifilic acid (TfOH, 1.5 equiv) was added, and the resulting reaction mixture was stirred for an additional 1 h. Upon completion of reaction, confirmed by thin layer chromatography (TLC) and mass spectrometry (MS), the reaction was quenched with pyridine (50 μL). The mixture was filtered, the filtrate was concentrated under reduced pressure, and the residue was purified by silica gel column chromatography using a gradient of hexanes and EtOAc (from 9/1 to 1/9, v/v) to give pure tetrasaccharide.

General Procedure for Synthesis of HS-Triazide Conjugates. Triazide conjugates (**1** or **2**) were prepared according to a previously reported procedure.[18] Briefly, to tetramers (**3** to obtain **1** or **4** to obtain **2**) in acetonitrile (0.5 mL for 1 mg) and DIPEA (4 equiv) at 0 °C was added an NHS-triazide linker (2 equiv, in 1.0 mL of acetonitrile). The progress of the reaction was monitored by ESI-MS. Upon completion, the reaction mixture was concentrated under vacuum and the residue obtained was purified by size exclusion chromatography (P-2 Biogel column). The appropriate fractions were lyophilized, and the residue was sodium exchanged over Dowex [Na +] resin.

The detailed synthetic procedures, NMR/MS characterization, and NMR spectra of all final compounds are provided in the Supporting Information.

Preparation of Peptide-Functionalized Surfaces. For DIBO coating on glass surfaces, DIBO-$(PEG)_3$-NH_2 (20 mM, DMF, 100 μL per well) was added to a multi-well hybridization cassette fitted with *N*-hydroxy succinimide (NHS)-activated glass slides (Nexterion Slide H). After 12 h incubation at room temperature in a closed chamber, the remaining activated esters were quenched with ethanolamine (5 mM) in Tris (100 mM) at pH 9.0. Azide-functionalized peptides were immobilized on the glass surface utilizing click chemistry. Briefly, peptides (100 μL per well, 0.5 mM or 1.0 mM in water, in triplicate) were added to the cassette, and after 16 h incubation, the solutions were removed, and the slides were rinsed with phosphate-buffered saline, spun dry, and kept in a desiccator at −20 °C for future use.

Preparation of HS Hydrogels. A premixed solution of DIBO-functionalized 4-arm PEG polymer (**8**, 7 wt %, 50 μL) and chimeric peptide (CP, final concentration of 1.0 mM) was added to an equal volume of synthetic HS-Triazide conjugate (stochiometric equivalent of **8**, 50 μL) in a ring-shaped PDMS mold (13 and 5 mm external/internal diameter and 5 mm height). After 30 min incubation at 37 °C, a stable hydrogel was obtained with a storage modulus of 0.5−1 kPa, which is in close agreement with a previous report.[18] The final composition of hydrogels is 3.5 wt % PEG polymer (**8**), 1.0 mM CP, and 7.25 mM HS (**1** or **2**).

Cell Culture. *Neural Stem Cell (NSC) Culture.* Human-induced pluripotent-derived neural stem cells (NSCs, Global Stem Cell, GSC-4306) were used. Cells were used at a passage ranging from P10 to P15. Cultures were expanded in a medium composed of neurobasal supplemented with glutamax (Gibco), non-essential amino acid (NEAA, Gibco), B27 (Gibco, ×50), and basic fibroblast growth factor (FGF2; R&D system). Differentiation of NSCs toward their committed lineage (*i.e.*, neurons, glia, and oligodendrocyte) was initiated using the same expansion media minus FGF2 (FGF2 withdrawal). Adhesion assays were performed over a period of 24 h post-seeding in maintenance media with FGF2 (initial seeding at 100k cells/cm^2). Both expansion and differentiation experiments in 3D were performed for a duration of 6 days (200k cells/10 μL of hydrogel).

Mel1-Derived PFC Neurons. For prefrontal cortical neural cell (PFC) differentiation, hESCs (Stem Cells Ltd., NIHhESC-11-0139) were dissociated on day 1 by EDTA and replated (260k/cm^2) on Matrigel-coated plates with Essential 8 Medium (Gibco). On day 0, the medium was replaced by Essential 6 Medium (Gibco) containing SB (10 μM, Tocris), LDN (100 nM, Selleck Chemicals), and XAV (2 μM, Tocris). From day 2 to day 8 (NPC induction), XAV was withdrawn from the medium. Day 8 NPCs were dissociated by a StemPro Accutase Cell Dissociation Reagent and replated as condensed droplets (10 drops into one well of a six-well plate) with homemade neural medium N2B containing N2 and B27 supplement (Gibco), FGF8 (50 ng/mL, R&D), and SHH (25 ng/mL, R&D) for neural rosette formation. On day 16, neural rosettes were dissociated by Accutase and replated (about two droplets into one well of a six-well plate) on PO/LM/FN-coated plates with N2B containing only FGF8. This was the final maintenance medium. On day 22, prefrontal cortical neural progenitors were dissociated by Accutase and replated (100k/cm^2) on PO (Sigma)/LM (R&D)/FN (VWR)-coated plates. PFC neurons were replated on 2D laminin-coated glass (100k/cm^2) or in gels (200k cells/10 μL of hydrogel) on day 30 for experiments as previously published.[21]

Recording of Neuronal Activity. *Microelectrode Array (MEA) Recordings.* For the MEA recordings, we used a 96-well MEA plate (BioCircuit MEA 96) coated with a mixture of PO (poly-orthine)/LM (laminin)/FN (Fibronectin). On day 22, Mil6-derived PFC neurons were dissociated by Accutase and replated (100k/cm^2) on the MEA plate in the final maintenance medium. Neuronal activity

https://doi.org/10.1021/acsami.2c01575
ACS Appl. Mater. Interfaces 2022, 14, 28476−28488

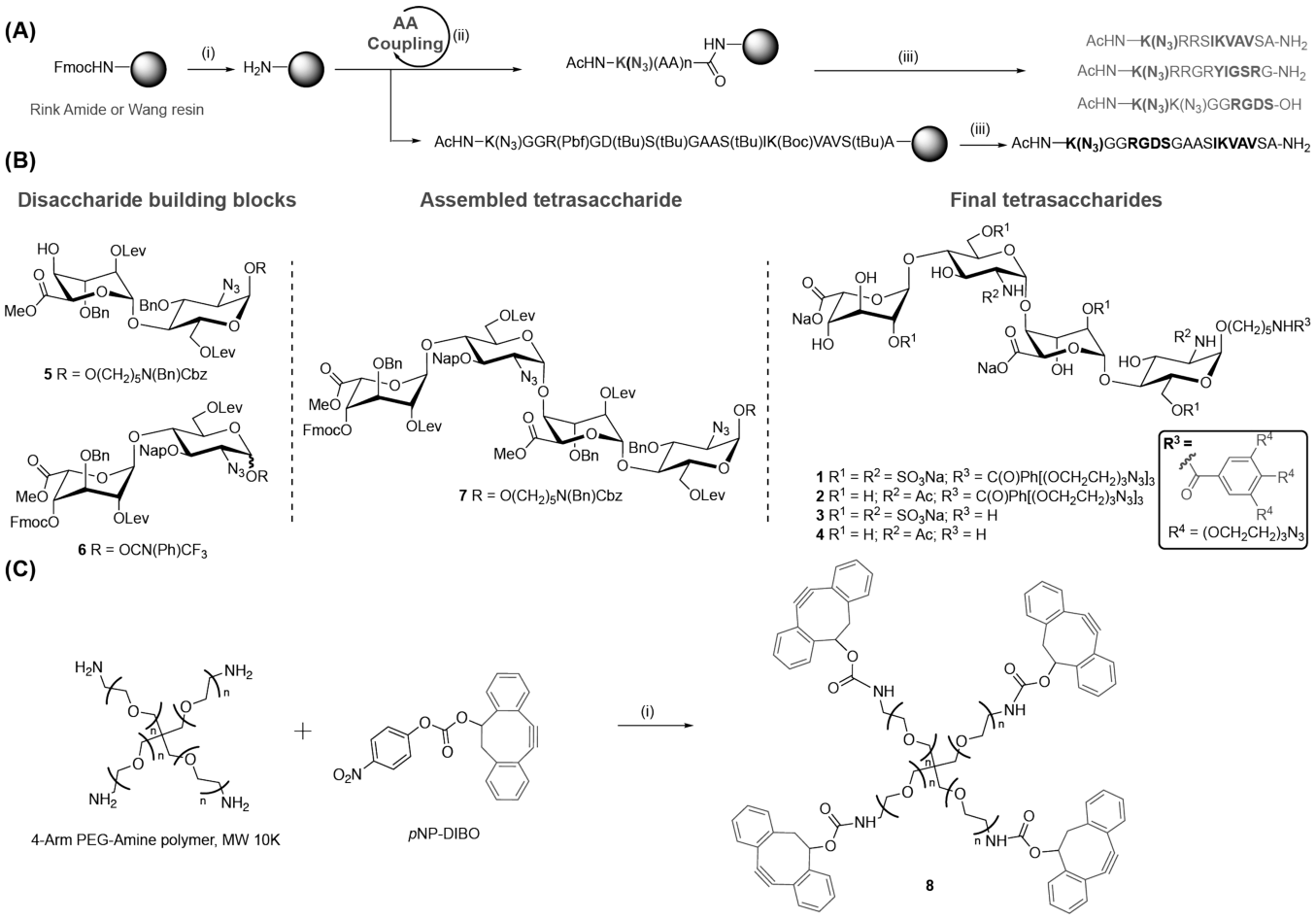

Figure 1. Chemical synthesis of HS-hydrogel components. (A) Microwave-assisted solid phase synthesis (MW-SPPS) of adhesion peptides. Reagents and conditions: (i) 20% 4-methylpiperidine, DMF, MW, 3 min; (ii) Fmoc-AA-OH, HOBt, HBTU, DIPEA, DMF, MW, 5 min; and (iii) TFA/H_2O/TIPS (95/2.5/2.5), RT, 2 h. (B) For modular synthesis of HS tetrasaccharides triazide conjugates (**1** and **2**) from their corresponding HS tetrasaccharides (**3** and **4**), disaccharide building blocks (**5** and **6**) were used to generate tetrasaccharide (**7**). Tetramer **7** was subjected to partial deprotection and then either to a sequence of O- and N-sulfation or N-acetylation followed by global deprotection to obtain **3** and **4**, which upon reaction with an NHS-activated triazide linker affords their corresponding triazide conjugates **1** and **2**, respectively. The Supporting Information provides the complete details of synthesis and analysis. (C) Synthesis of DIBO-functionalized 4-arm PEG polymer (**8**). Reagents and conditions: (i) DCM, Et_3N, 0 °C to RT, 16 h.

was recorded 1 week after replating using Maestro Pro (Axion Biosystems).

Calcium Imaging. Calcium imaging was performed using Fluo4-AM (Thermo-Fisher) using previously described methods.[22] Briefly, a stock solution was made using 50 μg of Fluo4-AM dissolved in 20% F127 Pluronic acid in DMSO (v/v). A loading solution was made from 2 mL of Brainphys and 4 μL of stock Fluo4-AM solution; cells were incubated for 20 min with the loading solution. Cells were then transferred to Brainphys only solution for recording. Following recording, hydrogels were changed back to regular maintenance media.

Calcium recording was performed on a Leica DM-IRBE inverted microscope with a fluorescence light source (Mercury Arc light source; Lumen dynamics) with a TRITC filter (Ex/Em: 561/576 nm). Following field of view centering using a 20× objective (NA: 0.4), imaging was performed for 5 min at 1 frame/s with 0.5 s exposure. Camera binning was further increased to 4 to allow a better signal-to-noise ratio. Cells were maintained in a Tokai live cell culture stage adapter maintained at 37 °C with a HEPA-filtered continuous flow of 5% CO_2-air medical-grade pre-mixed gas (Airgas).

Recorded time lapses (500 ms exposure, 1 frame/s) were then enhanced for contrast using Volocity software and exported as tiff image stacks. Cell somas were detected using maximum intensity projection, and regions of interest (ROI) were automatically defined using custom-made scripts in MATLAB with the image analysis toolbox. Calcium activity traces were extracted from ROI spatial average and plotted over time. Calcium spikes were detected using normalized $\Delta F/F$ and peak detection using MATLAB.

Protein Expression Quantification. *Western Blot Assays.* Sample protein concentrations were normalized to 30 μg of protein in 20 μL of PBS. A total of 7 μL of a 1:9 dilution of β-mercaptoethanol and Li-cor 4× Protein Loading Buffer was added to each sample before heating for 5 min at 95 °C. A total of 20 μL of each sample was run in duplicates on a Bio-Rad Mini-PROTEAN TGX gel at 200 V for 25 min in 1× TGS running buffer. Samples were transferred to a PVDF membrane at 15 V for 2 h in 1× Bio-Rad Trans-Blot Turbo Transfer Buffer + methanol. The membrane was washed in TBST and blocked in Li-cor Intercept Blocking Buffer overnight at 4 °C. The membrane was washed and then incubated with a 1:10,000 dilution of the primary antibodies (ERK1/2, P-ERK1/2, and GAPDH) in TBST + 5% BSA overnight at 4 °C. After washing, the membrane was incubated with a 1:15,000 dilution of the Li-cor IRDye 680 and 700 secondary antibodies in TBST + 5% BSA for 1 h at RT. The membrane was then washed, transferred to PBS, and kept in 4 °C until it was imaged on Li-cor Odyssey.

Immunocytochemical Staining. All cells were fixed in 4% paraformaldehyde (w/v in PBS) for 15 min. Following fixation, cells were washed with PBS and then with a 0.05% Tween-20 solution

https://doi.org/10.1021/acsami.2c01575
ACS Appl. Mater. Interfaces 2022, 14, 28476−28488

(Fischer Scientific; v/v in PBS). Cells were permeabilized using a 0.1% Triton-X100 solution (Fisher Scientific; v/v in PBS) and subsequently blocked in 4% BSA (Sigma Aldrich; w/v in PBS). Indicated primary and secondary antibodies were diluted in 2% BSA (w/v in PBS). Primary antibodies were applied to cells overnight at 4 °C. After washing with 0.05% Tween-20 (v/v in PBS), secondary antibodies were applied for 1 h at RT. All glasses or hydrogels were then counter-stained using DAPI/NucBlue nuclear staining and maintained in fluoromount-G solution (Thermo-Fisher), DAPI/Nucblue (Thermo Fisher, primary), Vinculin (Sigma Aldrich, 1:500/mouse, primary), Phalloidin-TX (Thermo Fisher, conjugated-TX), β-III-tubulin (EMD Millipore, 1:500/chicken, primary), Nestin (EMD Millipore, 1:500/mouse, primary), GFAP (DAKO, 1:500/rabbit, primary), Anti-mouse-AF488 (Life Technology, A11006, 1:220/goat, secondary), Anti-chicken-AF488 (Life Technology, A11039, 1:220/goat, secondary), and Anti-rabbit-AF647 (Life Technology, A21244, 1:220/goat, secondary).

Image Quantification. Quantification for DAPI-based cell nucleus count, cell membrane staining area, and colocalization were performed using a custom-made script using MATLAB (MathWorks, Inc.) and an image analysis toolbox. Differentiation index in each condition was estimated as the ratio of the cumulative number of differentiated cells (B3T+ and GFAP+) and the total number of cells (NESTIN+).

HS Interaction with FGFR1 and FGF2. Compounds **1** and **2** (with azide groups, 100 μM, in water) were added to a multi-well hybridization cassette (100 μL per well, in triplicate) fitted with a DIBO-functionalized glass slide. After 1 h incubation at RT, the excess solutions were removed, rinsed with PBS, and spun dry. Similarly, 100 μM solutions of compounds **3** and **4** bearing an anomeric amino pentylamine linker were added on to NHS-ester-activated glass slides (Nexterion Slide H). After 8 h, the slides were incubated in a humidity chamber for 16 h and then blocked for 1 h with ethanolamine (5 mM) in a Tris buffer (pH 9.0, 50 mM) at RT for 1 h. The blocked slides were rinsed with deionized water and spun dry. First, HS-functionalized slides were incubated with FGF2 (R&D systems, 3 μg/mL). After 1 h at RT, the slide was sequentially washed by dipping in TSM wash buffer (2 min, with 0.05% Tween 20), TSM buffer (2 min), water (2 × 2 min), and spun dry. For detection of bound protein, the slide was incubated with anti-FGF2 (1:300) followed by goat anti-mouse Alexa Fluor 635 (1:300) in the dark. The slide was scanned using a GenePix 4000B microarray scanner (Molecular Devices) at the 635 nm excitation wavelength. Next, fresh slides were incubated with FGFR1 (Sino Biological, 10 μg/mL) with and without FGF2 (R&D systems, 3 μg/mL) for 1 h at RT. The same sequence of washing was repeated, and the slide was further incubated with anti-His-AlexaFluor-635 (BioLegend, 5 μg/mL) in the dark. Following the washing steps, the slide was scanned, and the data was plotted using Prism GraphPad software.

Statistical Analysis. All statistical analyses were performed using MATLAB (MathWorks, Inc.) and the statistical toolbox. For all validating normality tests (Kolmogorov–Sinai test), parametric methods including *t*-tests and ANOVA were used with a Holm–Sidak correction for multiple comparison when appropriate. Otherwise, non-parametric methods such as the Wilcoxson ranksum test and Kruskal–Wallis test with Dunn–Sidak correction for multiple comparison were used.

RESULTS AND DISCUSSION

The biomimetic attributes of tissue-engineered synthetic HS constructs that are designed to enhance FGF2 signaling and promote NSC and neuronal homeostasis have so far not been fully characterized. In a previous study, we demonstrated that different arrangements of synthetic sulfated HS disaccharides in an HS backbone can exhibit distinct structure–function attributes.[23] We also reported that 3D hydrogel constructs presenting these epitopes potentiated FGF2 activity and promoted NSC proliferation.[18] Here, we formulated a general strategy to incorporate an HS tetrasaccharide and a chimeric peptide into a three-dimensional matrix using strain-promoted alkyne-azide cycloaddition (SPAAC) chemistry to promote cell proliferation and differentiation (Figure 1). First, we evaluated NSC adhesion to a hybrid chimeric peptide, laminin, and laminin sub-domain peptides in a 2D configuration. Next, the binding of synthetic HS tetrasaccharides to FGF2 and its corresponding receptor, FGFR, was examined. Finally, the impact of HS sulfation and the presence of the chimeric peptide in a 3D scaffold on NSC's fate and neuronal activity were examined. We prepared azido-functionalized integrin binding peptides (RGDS, YIGSR, and IKVAV) and chimeric peptides that contained the integrin binding regions RGDS and IKVAV and covalently linked them to dibenzocyclooctyne (DIBO)[24]—modified glass surfaces or a polymeric backbone via SPAAC chemistry. Following a modular approach for HS synthesis,[25] a high affinity fully sulfated and control unsulfated tetrasaccharides were prepared. The HS tetrasaccharide bears an anomeric amino pentyl linker, which can be used for attachment of a tri-azido linker[18] for hydrogel formation or can be printed on the glass slide for FGF2/FGFR1 binding studies.

Preparation of HS Hydrogel Components. To incorporate adhesive peptides into HS-hydrogel scaffolds, we utilized a pendant approach to ensure relevant 3D presentation of peptides for functional interactions. For conjugation to a scaffold, the N-terminus of the peptides was modified by an amino acid having an azido-containing side chain. Additional amino acids were introduced in the sequence to facilitate aqueous solubility and to confirm suitable spacing between the integrin-binding domain and the hydrogel backbone (Figure 1A). The peptide synthesis was performed by microwave-assisted solid phase peptide synthesis (MW-SPPS) using *N*-α-Fmoc-protected amino acids and 2-(1*H*-benzotriazole-1-yl)-1,1,3,3-tetramethyluronium hexafluorophosphate (HBTU)/1-hydroxybenzotriazole (HOBt) as the activating reagents. After cleavage from the resin, the peptides were purified by reverse-phase HPLC and characterized by mass spectrometry (MALDI-ToF MS).

We selected a fully sulfated HS tetrasaccharide **3** that is known to support FGF2 mitogenic signaling in BaF3 cells transfected with FGFR1c.[19] In addition, a tetrasaccharide **4** lacking sulfates was employed as a negative control. For the synthesis of HS tetrasaccharides **3** and **4**, an acid-mediated glycosylation reaction of disaccharide acceptor **5** with disaccharide donor **6** provided a tetrasaccharide **7** (Figure 1B and Figure S1). The levulinoyl (Lev) esters of **7** could selectively be removed by treatment with hydrazine acetate, and the resulting hydroxyls were sulfated using the sulfur trioxide/pyridine complex (SO_3/Py). Next, the methyl esters were saponified and the azido groups were reduced to amines, which were either N-sulfated or N-acetylated and then subjected to hydrogenation to afford the target tetrasaccharides **3** and **4**. To obtain triazide-functionalized tetrasaccharides (**1** and **2**), the NHS-activated tri-azido PEG linker (**S5**, Figure S1) was coupled with the anomeric linker amine group of **3** and **4**, respectively.

For the preparation of DIBO-functionalized 4-arm PEG (**8**, Figure 1C), commercially available 4-arm PEG-amine (mol. wt.: 10 KDa, Creative PEGWorks) was coupled with *p*-nitrophenyl carbonate of DIBO in the presence of Et_3N and the product was purified by size exclusion chromatography over an LH-20 column (CH_2Cl_2/CH_3OH, 1/1, v/v). All the compounds were fully characterized by mass spectrometry

https://doi.org/10.1021/acsami.2c01575
ACS Appl. Mater. Interfaces 2022, 14, 28476–28488

(MS) and nuclear magnetic resonance (NMR) (Experimental Procedures in the Supporting Information).

Peptide-Functionalized 2D Glass Surfaces for Cell Adhesion Assays. Azido-functionalized chimeric peptide (CP, Figure 2A) was immobilized to glass slides modified by

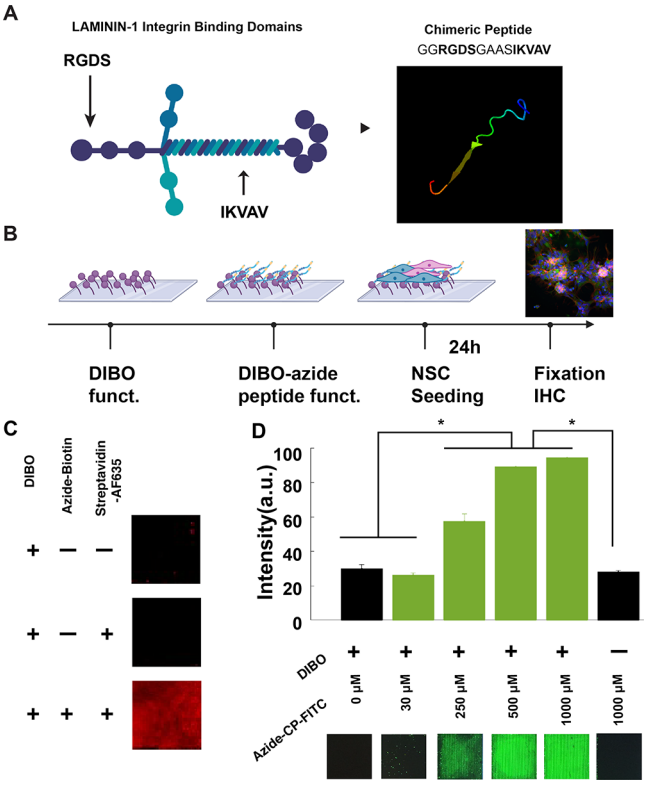

Figure 2. DIBO functionalization allows controlled peptide coating of 2D glass for the adhesion assay. (A) Integrin binding sites of laminin-1 can be combined in a shorter efficient chimeric peptide that promotes cellular adhesion to a surface. We used a chimeric peptide (CP) previously designed for enhanced cell adhesion combining RGDS and IKVAV. The laminin graphic was created by biorender.com. Inset: the I-TASSER protein model is shown. (B) Functionalization steps include covalent attachment of amine-$(PEG)_3$-DIBO to the NHS-activated glass slide followed by a click-reaction of various concentrations of azide-modified peptides. Post-functionalization, human-induced pluripotent (hIP)-derived neural stem cells (NSCs) were seeded for attachment. The summary graphic was created by biorender.com. (C) Validation of DIBO group attachment to a glass surface. The presence of DIBO is confirmed by sequential addition of biotin-azide and streptavidin-AlexaFluor-635. Fluorescence was observed only when all required components are present. (D) Validation of CP functionalization on a glass slide using a fluoresceine-modified azide-CP (FL-azide-CP, top panel). Concentration-dependent binding of adhesion peptide; triplicates for each condition. * indicates $p < 0.05$. Representative fluorescence intensity for each concentration-dependent binding of FL-azide-CP (bottom panel). The error bars indicate ± s.e.m.

DIBO using a range of different concentrations to determine the optimal density for hNSC cell adhesion. hNSCs were allowed to adhere to the surfaces for a period of 24 h, after which they were fixed and stained with relevant neural cell markers (Figure 2B). The uniformity of DIBO functionalization was confirmed by sequential treatment of the surfaces with biotin-azide and streptavidin-AlexaFluor-635 followed by fluorescence scanning (Figure 2C). A chimeric peptide having a lysine residue modified by fluorescein (FL) was also conjugated to validate covalent coupling of azide-CP to DIBO glass surfaces. An increase in fluorescence intensity was observed for increasing concentrations of chimeric peptide (Figure 2D), confirming the azide-CP concentration-dependent immobilization to DIBO glass surfaces. Next, we functionalized the glass slides with unmodified chimeric peptide and quantified hNSC adhesion by counting DAPI+ nuclei. These results indicate the chimeric peptide concentration-dependent enhancement of hNSC adhesion (Figure 3A1−A4,D; DAPI staining). Adherent hNSCs also demonstrated the chimeric peptide concentration-dependent enhancement in percent area of focal adhesion protein Vinculin (Figure 3B2,C2,E) and filamentous actin presence as marked by Phalloidin (Figure 3B3,C3,E).

hNSCs were seeded on chimeric peptide-modified surfaces (1 mM concentration), and the number of cells was quantified 24 h post-seeding using DAPI+ staining and Vinculin + Phalloidin + colocalization. Results indicated comparable levels of cell adhesion to laminin-coated surfaces (20 μg/mL; Figure S2A−E). Similar results were obtained using RGDS peptide-functionalized surfaces (Figure S2D,E). However, IKVAV peptide-functionalized surfaces failed to elicit similar effects (Figure S2D,E, $p > 0.05$). The degree of hNSC adhesion to chimeric peptide-functionalized glass showed a non-linear dependency on peptide concentration (Figure 3A−E). We detected the significantly greater adhesion of hNSCs on 2D substrates containing peptide concentrations above 250 μM (Figure 3D,E; $p < 0.05$). These results indicated that the chimeric peptide-modified 2D surfaces promoted neural cell adhesion that is comparable to laminin.

Ternary Complex of FGFR1, FGF2, and HS Tetrasaccharide. To evaluate whether **1** and **2** can bind to FGF2 as well as FGFR1, we tested FGF2 and FGFR1 binding to **1**- and **2**-functionalized glass slides (Figure 4A). Bound FGF2 and his-tagged FGFR1 were detected by using anti-FGF2 and anti-his antibodies, respectively (Figure 4 and Figure S3). The results indicated that SPAAC-immobilized **1** showed a significantly higher affinity for FGF2 when compared to SPAAC-immobilized **2** (Figure 4B, $p < 0.01$). To investigate whether immobilized HS can form a ternary complex with FGF2 and FGFR1, we used printed arrays functionalized with **1** and **2** with and without FGF2 (50 ng/mL; Figure 4C). FGFR1 was found to bind only to immobilized **1** as detected via anti-His-AlexaFluor-635 antibody binding (Figure 4C). Importantly, the binding was significantly enhanced in the presence of FGF2 on the printed array (Figure 4C; two-way anova, $p < 0.05$; factor sulfation, $p < 0.001$; factor FGF2, $p < 0.001$; **1** no FGF2 vs FGF2: $p < 0.001$) as well as with amine-conjugated HS tetrasaccharides (Figure 4D; right panel; $p < 0.001$; compounds **3** and **4**). Collectively, these results indicated that **1** can engage with both FGF2 and FGFR1 to form a ternary complex.

FGF2 plays an important role in promoting proliferation and maintenance of stemness.[26] Following FGF2 withdrawal, NSCs lose self-renewal properties and demonstrate reduced viability and increased differentiation to neurons, astrocytes, and oligodendrocytes.[27] HS interacts with FGF2 in a sequence and sulfation-selective manner and regulates FGF2 presentation to adherent cells *via* the formation of a co-receptor complex.[28] Crystallographic[29] and NMR[20] studies have shown that a tri-sulfated IdoA2S-GlcNS6S motif can bind to FGF2 and that a hexa- and octasaccharide can form stable ternary

https://doi.org/10.1021/acsami.2c01575
ACS Appl. Mater. Interfaces 2022, 14, 28476−28488

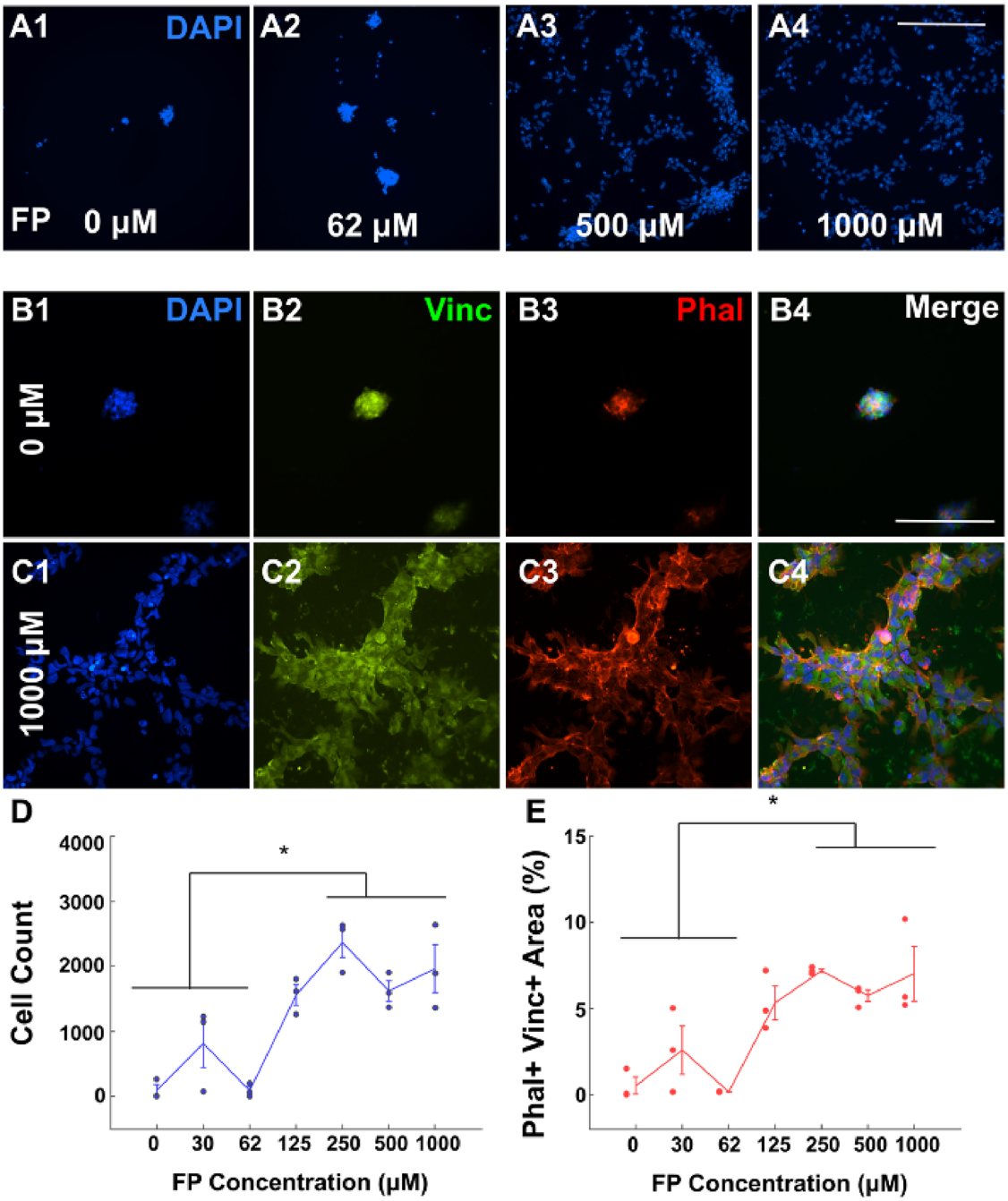

Figure 3. Concentration-dependent adhesion of NSCs to chimeric peptide. (A) Representative figure showing the NSC presence 24 h post-seeding with DAPI staining for 0 μM (A1), 62 μM (A2), 500 μM (A3), and 1000 μM (A4) CP-coated glass. Scale bar: 500 μm. (B) Representative image showing the cell presence 24 h post-seeding for 0 μM CP-coated glass (negative control); DAPI (B1, blue), Vinculin (B2, green), Phalloidin-TX (B3, red), and merge channels (B4) are shown. Scale bar: 100 μm. (C) Representative image showing the cell presence 24 h post-seeding for 1000 μM CP-coated glass; DAPI (C1, blue), Vinculin (C2, green), Phalloidin-TX (C3, red), and merge channels (C4) are shown. Scale bar: 100 μm. (D) Count for DAPI+ cells in each condition. (E) Area coverage of Phalloidin+ and Vinculin+ as a percentage of the total image area for DAPI+ cells in each condition. * indicates $p < 0.05$. All experiments are performed in triplicates for each condition. The error bars indicate ± s.e.m.

complexes with FGF2 and FGFR1.[30] Moreover, a tetrasaccharide when introduced exogenously to EXT-1$^{-/-}$ mouse lung endothelial cells restored cellular function by acting as a co-receptor to facilitate FGF2 binding to FGFR1.[31] Our findings demonstrate that the fully sulfated HS tetrasaccharide (**1**), which is composed of IdoA2S-GlcNS6S repeating units, can engage with both FGF2 and FGFR1 to form a ternary complex when compared to unsulfated HS (**2**). These results corroborate previous reports describing the ability of synthetic HS oligosaccharides to function as co-receptors[8,32] and underscore the role of HS sulfation in trophic factor stabilization.[18,33]

Effect of HS Sulfation and Chimeric Peptide Presentation in 3D Hydrogels on Cell Differentiation and Extracellular Signal-Regulated Kinase (ERK) Signaling. To evaluate the effect of HS sulfation and chimeric peptide presentation on mitogen signaling, we encapsulated hNSCs in 3D HS hydrogels obtained by mixing stoichiometric

https://doi.org/10.1021/acsami.2c01575
ACS Appl. Mater. Interfaces 2022, 14, 28476−28488

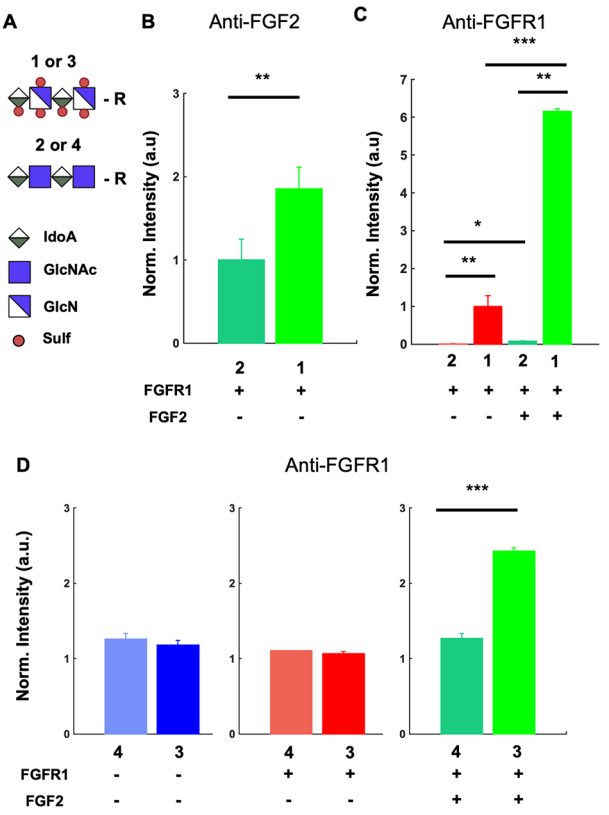

Figure 4. Fully sulfated HS tetrasaccharides form a ternary complex with FGF-2 and FGFR. (A) Fully sulfated HS (**1** or **3**) and a control tetrasaccharide lacking sulfation (**2** or **4**). R represents the anomeric linker, R = $O(CH_2)_5NHCO[Ph(O\text{-}PEG\text{-}N_3)_3]$ for **1** and **2** covalent attachments to the DIBO-functionalized glass slide and R = $O(CH_2)_5NH_2$ for **3** and **4** printing on the NHS-activated glass slide. (B) Fluorescence intensity from sub-arrays modified with **1** (100 μM) and **2** (100 μM), incubated with FGF-2 (3.0 μg/mL). Bound FGF-2 was detected by first incubating with anti-FGF2 antibody (1:300) followed by anti-rabbit-AlexaFluor-647 (1:300). ** indicates $p < 0.01$. Intensity values in **1** were normalized relative to **2**. (C) Fluorescence intensity from sub-arrays printed with **2** (100 μM) and **1** (100 μM), incubated with His-tagged FGFR1 (10.0 μg/mL). Bound FGFR1 was detected using anti-His-tag-AlexaFluor-635 (5.0 μg/mL). ** indicates $p < 0.01$. (D) Fluorescence intensity from sub-arrays modified with **4** (100 μM) and **3** (100 μM), incubated with His-tagged FGFR1 (10.0 μg/mL). Bound FGFR1 was detected using anti-His-tag-AlexaFluor-635 (5.0 μg/mL); after washing, the remaining fluorescence would indicate the presence of FGFR1. * indicates $p < 0.05$. Intensity normalized relative to no HS control. All experiments were performed in triplicates (SPAAC arrays) or six replicates (printed arrays) for each condition. The error bars indicate ± s.e.m.

quantities of HS-tri-azido (**1** or **2**) and chimeric peptide-modified DIBO-functionalized 4-arm PEG polymer (**8**) (Figure 1A and Figure S4). Next, we quantified the cellular expression of the stemness marker Nestin (Nest; Figure 5A and Figure S5), the neuronal marker β-III Tubulin (B3T; Figure S5), and the astrocyte marker Glial fibrillary acidic protein (GFAP; Figure S5) in hNSCs encapsulated in **1**/**2** hydrogels with or without chimeric peptide for 6 days *in vitro*. hNSCs encapsulated in **2**-CP hydrogels and cultured in the presence of FGF2 (Figure 5) demonstrated a greater neuronal differentiation as marked by the β-III Tubulin (B3T+) signal (Figure 5C; **2**-CP vs all, $p < 0.05$; Figure S5C) when compared to other conditions, with marginal differentiation toward astrocytes (Figures S5 and S6C). Interestingly, it was found that the number of Nestin+ cells was significantly higher in **2** (Figure 5A1,B; two-way ANOVA, interaction factor, $p < 0.05$; post-hoc, **2** vs **2**-CP, $p < 0.05$) and **1**-CP (Figure 5A4,B; **1**-CP vs **2**-CP, $p < 0.01$; **1**-CP vs **1**, $p < 0.05$) conditions compared to **1** and **2**-CP.

Western blot analysis of phosphorylated-ERK1/2 (p-ERK1/2) expression in hNSCs (Figure 5E and Figure S7) was conducted to validate the downstream effects of HS-mediated FGF2 and FGFR1 complexation studies (Figure 4). Results indicated that the ratio of p-ERK1/2 to ERK1/2 was enhanced in the presence of FGF2 in 2D hNSC cultures (Figure 5F). Interestingly, we also detected a significantly higher p-ERK1/2 ratio in hNSCs encapsulated in **2** and **1**-CP when compared to hNSCs encapsulated in **1** and **2**-CP hydrogels (Figure 5F; two-way ANOVA, interaction factor, $p < 0.05$; **2** vs **1**/**2**-CP: $p < 0.05$; **1**-CP vs **1**/**2**-CP: $p < 0.05$). These observations indicated that the sulfation pattern of HS can modulate neuronal differentiation relative to the presence of adhesion peptide. We then encapsulated hNSCs in **1**- and **2**-containing hydrogels as well as similar preparations incorporating chimeric peptide (**1**-CP/**2**-CP) and cultured these in the absence of FGF2 to investigate the effects on cell differentiation (Figure 6 and Figure S6B). Quantification of the neural markers Nest, B3T, and GFAP at day 6 post-seeding indicated a significantly higher neuronal differentiation of hNSCs encapsulated in chimeric peptide-functionalized **1** and **2** hydrogels (Figure 6E,G; two-way ANOVA, adhesion factor CP vs no CP, $p < 0.001$). However, no significant changes in GFAP expression were observed (Figure S6C; two-way ANOVA, all factor $p > 0.05$). We did not detect an effect of sulfation in the absence of FGF2 (sulfation factor, $p > 0.05$). These results demonstrated that chimeric peptide-functionalized HS hydrogels can promote and sustain a strong neuronal differentiation of hNSCs in the absence of FGF2.

Peptide motifs in neural cell adhesion proteins such as fibronectin and N-cadherin have been reported to promote FGF2 signaling[16,17] as well as the migration and proliferation of NSCs.[15] Phosphorylation of extracellular regulated kinase 1 and 2 (pERK1/2) regulates stem cell multipotency and is activated by HS-mediated ternary complex formation with FGF2-FGFR.[34] A higher pERK1/2 ratio indicates a greater stemness and reduced differentiation potential. Interestingly, our results indicated that pERK1/2 was significantly reduced along with an overall reduction in Nestin expression in hNSCs encapsulated in **1** hydrogels that lacked cell adhesion-promoting chimeric peptide. In contrast to hNSCs in **1**, hNSCs in **2** hydrogels lacking chimeric peptide exhibited significantly higher p-ERK1/2 levels and higher Nestin expression. These results led us to speculate that although fully sulfated **1** hydrogels facilitated ternary complex formation, the absence of cell adhesive chimeric peptide might have caused a greater sequestration of FGF2 by HS, leading to reduced stem cell proliferation and pERK1/2 expression in encapsulated hNSCs. Further supporting evidence for this was obtained from subsequent experiments involving hNSCs encapsulated in chimeric peptide-functionalized **1** hydrogels (**1**-**CP**), which demonstrated significantly enhanced p-ERK1/2 levels and higher Nestin expression. We did not observe a statistically significant difference in pERK levels in hNSCs encapsulated in chimeric peptide-lacking hydrogels (**1**) and chimeric peptide-containing **2** hydrogels (**2**-**CP**) and therefore cannot attribute the enhanced B3T expression and neuronal

https://doi.org/10.1021/acsami.2c01575
ACS Appl. Mater. Interfaces 2022, 14, 28476−28488

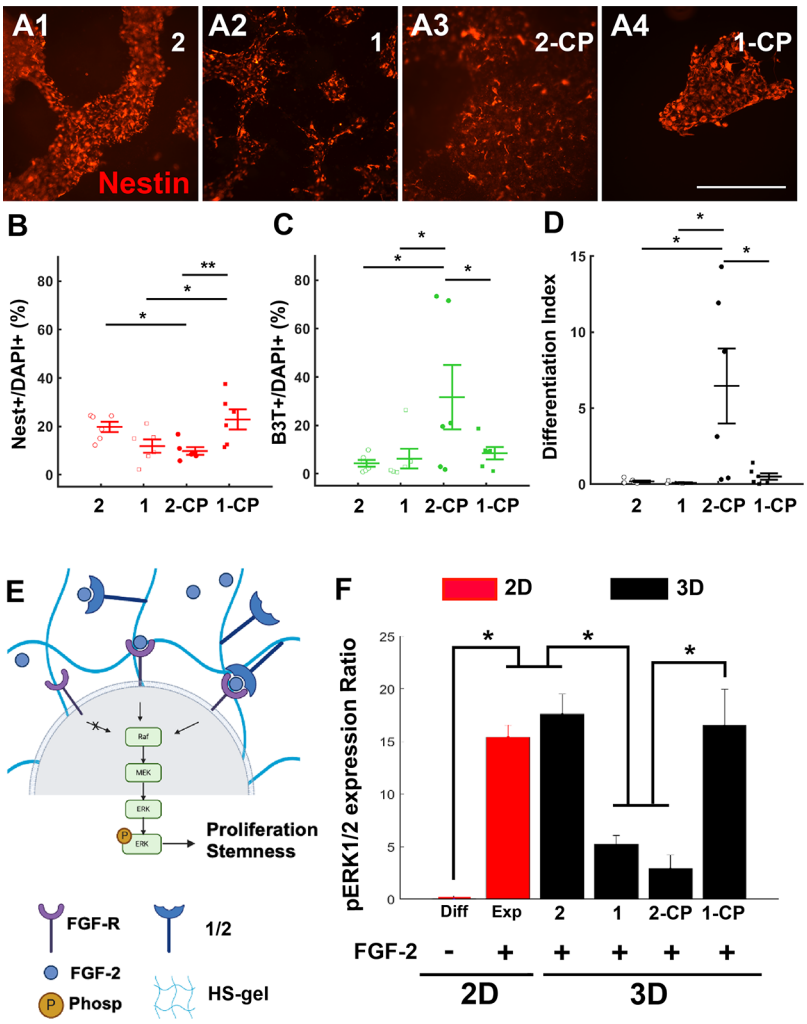

Figure 5. Heparan sulfate-chimeric peptide-mediated regulation of NSC maintenance. (A) Representative images showing Nestin staining of NSCs at week 1 post-seeding in HS hydrogels with **2** (A1), **1** (A2), **2**-CP (A3), and **1**-CP (A4) conditions. Scale bar: 500 μm. (B) Nestin+ cells as a percentage of DAPI+ in each condition. (C) B3T+ cells as a percentage of DAPI+ in each condition. (D) Differentiation index in each condition is estimated as the ratio of the cumulative number of differentiated cells (B3T+ and GFAP+) and the total number of cells (DAPI+). (E) FGF-2 binding to its receptor FGFR triggers the downstream expression of the Raf-MEK-ERK1/2 pathway. Phosphorylation of ERK1/2 results in cellular proliferation and maintenance of stemness. The summary graphic was created by biorender.com. (F) Quantified p-ERK1/2 to ERK1/2 ratio. 2D condition (red) used laminin (20 μg/mL) as the cell adhesion substrate. 3D HS-GAG (black) condition used CP (1 mM) the cell adhesion substrate. * indicates $p < 0.05$. All experiments were performed in six replicates for each condition. The error bars indicate ± s.e.m.

differentiation of cells in **2-CP** solely to reduced pERK levels. We speculate that the enhanced cell adhesion due to the presence of CP might drive a greater neuronal differentiation (and B3T expression) of cells in **2-CP**. To summarize these findings, we conclude that the presence of FGF2 alone is sufficient to promote stemness and reduce differentiation in the absence of both CP and fully sulfated HS. However, FGF2 alone is not sufficient to promote stemness in the presence of either fully sulfated HS or CP, indicating that the chimeric peptide and fully sulfated HS are required to function synergistically to enhance FGF2-mediated hNSC stemness.

Chimeric Peptide Supports Long-Term Neural Activity. Since cell adhesion is essential to promote the survival and activity of differentiated neurons, we tested the ability of chimeric peptide-functionalized HS gels to support neural activity in differentiated neurons. We used pre-differentiated neurons from human embryonic stem cells (Mel-1 hESCs; Figure 7A) for these assays, and neuronal activity was quantified using the intracellular calcium indicator dye Fluo-4AM at day 7 post-seeding (Figure 7B,C). These pre-differentiated neurons are known to exhibit spontaneous activity at week 1 post-seeding.[21] Neurons were seeded on microelectrode arrays (MEA) and on laminin-coated glass to obtain baseline activity levels on validated 2D substrates using electrophysiological recordings and calcium imaging (Figure 7B), respectively (Figure 7A, right panel). Neuronal recordings were obtained 7 days post-seeding in all conditions including in chimeric peptide-functionalized HS (Figure 7A). Conditions lacking chimeric peptide were not assessed as they do not provide optimal conditions for survivability for pre-differentiated neurons.[35] We found that on MEA, the seeded neurons showed a high percentage of activity (Figure 7D; ~100% of all eight electrodes had neuronal spikes) with an average firing frequency of 14.7 spikes/min (Figure 7E). MEA recordings provide the activity profiles of neuron clusters as they do not have sufficient spatial resolution for single neuron activity, resulting in a higher activity and firing frequencies. Using Fluo4-AM on cells seeded on 2D substrates, the

https://doi.org/10.1021/acsami.2c01575
ACS Appl. Mater. Interfaces 2022, 14, 28476−28488

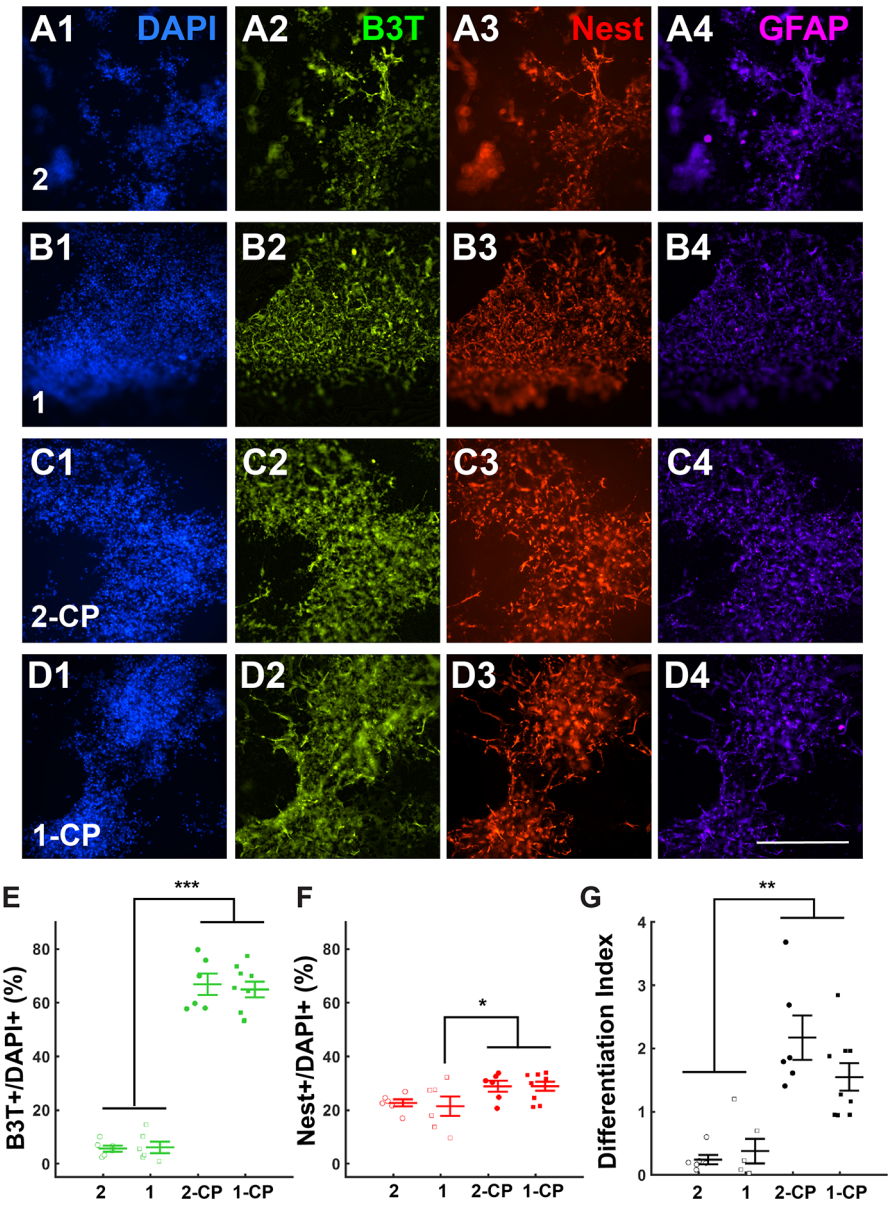

Figure 6. NSCs differentiated into neurons only in chimeric peptide-functionalized HS constructs and in the absence of FGF-2. (A) Representative images showing lineage commitment of NSCs 1 week post-seeding in the 3D HS hydrogel with **2**; DAPI (A1), BIII-Tubulin (A2), Nestin (A3), and GFAP (A4) staining are shown. (B) Representative images showing lineage commitment of NSCs 1 week post-seeding in the 3D HS hydrogel with **1**; DAPI (B1), BIII-Tubulin (B2), Nestin (B3), and GFAP (B4) staining are shown. (C) Representative images showing lineage commitment of NSCs 1 week post-seeding in the 3D HS hydrogel with **2**-CP; DAPI (C1), BIII-Tubulin (C2), Nestin (C3), and GFAP (C4) staining are shown. (D) Representative images showing lineage commitment of NSCs 1 week post-seeding in the 3D HS hydrogel with **1**-CP; DAPI (D1), BIII-Tubulin (D2), Nestin (D3), and GFAP (D4) staining are shown. Scale bar for (A–D): 500 μm. (E) B3T+ cells as a percentage of DAPI+ in each condition. (F) Nestin+ cells as a percentage of DAPI+ in each condition. *** indicates $p < 0.001$. (G) Differentiation index in each condition. * indicates $p < 0.05$. All experiments were performed in six replicates for each condition. The error bars indicate ± s.e.m.

validated % of active cells (Figure 7D; percentage of cells showing at least one spike within 5 min out of all detected cells) was found to be ∼48% with an average firing frequency of 1.0 spikes/min. Interestingly, both **2**-CP- and **1**-CP-hydrogel encapsulated cells showed a similar range of activities (Figure 7D; **2**-CP; **1**-CP; one-way ANOVA on Fluo4, $p > 0.05$) and firing rate (Figure 7E; **2**-CP: 0.7 spikes/min; **1**-CP: 0.6 spikes/min; one-way ANOVA on Fluo4, $p > 0.05$) compared to neurons seeded on 2D substrates. These results indicated that CP-functionalized HS hydrogels can sustain long-term neuronal development and support the maturation of active neurons.

These results demonstrated that **2**-CP hydrogels can support cell adhesion-dependent neuronal differentiation of hNSCs solely via chimeric peptide activity. Neuronal cell adhesion-promoting peptide motifs were found to be essential to support neuronal differentiation in the presence and absence of FGF2 and can function synergistically along with FGF2 binding fully sulfated HS motifs presented in **1**-CP hydrogels to support ternary complex formation and FGF2-mediated self-renewal of hNSCs. Taken together, the modularity of our hydrogel constructs demonstrates the functional importance of tailoring cell adhesive peptides and sulfation patterns to regulate hNSC

https://doi.org/10.1021/acsami.2c01575
ACS Appl. Mater. Interfaces 2022, 14, 28476−28488

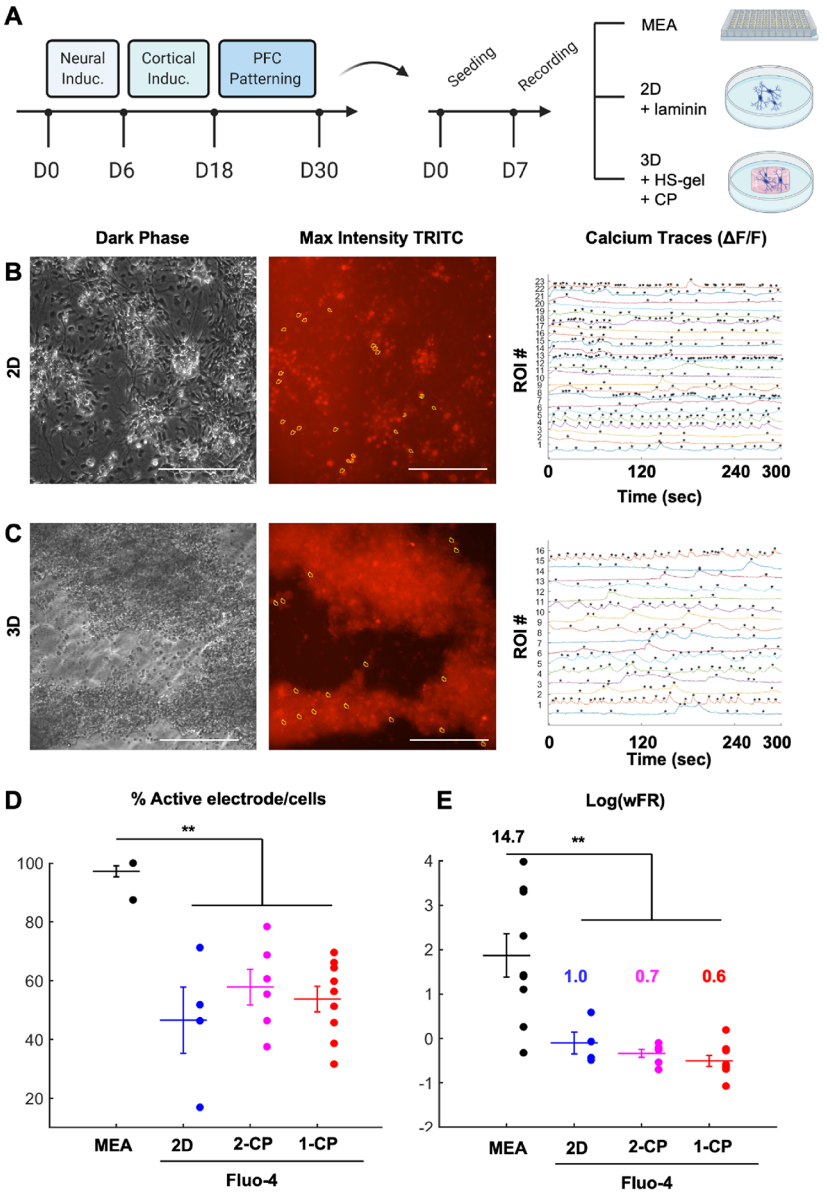

Figure 7. Chimeric peptide-functionalized HS hydrogels support the long-term activity of a neuronal network. (A) Experimental schedule showing PFC neuron differentiation steps from Mil6 human embryonic stem cells. At day 30 of differentiation, cells are reseeded in either MEA plates, 2D glass bottom plates (laminin; 20 μg/mL), or HS hydrogel with chimeric peptide (1 mM; **1** and **2**). The summary graphic was created by biorender.com. (B) Representative 2D culture of PFC neurons showing the dark field image (left), maximum intensity (TRITC, middle), and extracted calcium traces from Fluo4-AM recorded time lapses (right). Total recording duration: 5 min. * indicates the detection of a calcium spike from the $\Delta F/F$ processed traces. Scale bar: 100 μm. (C) Representative 3D culture of PFC neurons (**1**-CP) showing the dark field image (left), maximum intensity (TRITC, middle), and extracted calcium traces from Fluo4-AM recorded time lapses (right). Total recording duration: 5 min. * indicates the detection of a calcium spike from the $\Delta F/F$ processed traces. Scale bar: 100 μm. (D) Estimated % of active sites from recording. An active site was designated for an electrode or an ROI showing at least one spike during the 5 min recording. ** indicates a $p < 0.01$. (E) log of the weighted firing rate (wFR). wFR was estimated as the average firing rate in spikes/min from the active electrodes or ROI obtained from MEA and Fluo4-AM recordings, respectively. Inset numbers indicate the wFR for each condition. ** indicates a $p < 0.01$. All experiments were performed in 8, 4, 6, and 9 replicates for the MEA, 2D, 3D 2-CP, and 3D 1-CP, respectively. Error bars indicate ± s.e.m.

maintenance and differentiation in 3D tissue engineered scaffolds.[36]

CONCLUSIONS

We describe a modular strategy to integrate the presentation of fully synthetic sulfated HS tetrasaccharides with neuronal adhesion peptides in 3D hydrogels that can be used to evaluate the influence of these cues on cell−extracellular matrix interactions and FGF2 signaling. Although we did not evaluate the influence of the precise sulfation pattern of an HS oligosaccharide on functional properties, the results presented here provide proof-of-concept that well-defined sulfated synthetic heparan sulfate oligosaccharides can be employed to examine their influence on growth factor signaling and cellular homeostasis. In this study, a sulfated HS tetrasaccharide was selected based on the observation that it can transiently stabilize the FGF2-FGFR1 complex.[19,20] A fully sulfated disaccharide does not exhibit these properties and binds with lower affinity to FGF2, thereby only providing

https://doi.org/10.1021/acsami.2c01575
ACS Appl. Mater. Interfaces 2022, 14, 28476−28488

thermal stability.[18] To our knowledge, this is the first demonstration of 3D synthetic HS and adhesion peptide-functionalized constructs that elicit physiologically relevant interactions with FGF2 and FGFR1 to modulate hNSC proliferation and neuronal differentiation. Future studies will focus on the improved hydrogel presentation of bioactive components and cellular characterization of encapsulated cells.

■ ASSOCIATED CONTENT

Supporting Information

The Supporting Information is available free of charge at https://pubs.acs.org/doi/10.1021/acsami.2c01575.

Additional experimental details, materials, and methods, including 2D adhesion assays (SPAAC functionalization), 3D representative figures, additional quantifications (DAPI+ and GFAP+ cells), Western blots, and 1D/2D NMR spectrums (PDF)

■ AUTHOR INFORMATION

Corresponding Authors

Geert-Jan Boons − *Complex Carbohydrate Research Center and Department of Chemistry, University of Georgia, Athens, Georgia 30602, United States; Department of Chemical Biology and Drug Discovery, Utrecht Institute for Pharmaceutical Sciences, and Bijvoet Center for Biomolecular Research, Utrecht University, Utrecht 3583, The Netherlands;* orcid.org/0000-0003-3111-5954; Email: gjboons@ccrc.uga.edu

Lohitash Karumbaiah − *Regenerative Bioscience Center, Edgar L. Rhodes Center for ADS, College of Agriculture and Environmental Sciences, and Division of Neuroscience, Biomedical and Translational Sciences Institute, University of Georgia, Athens, Georgia 30602, United States;* orcid.org/0000-0001-7969-417X; Email: lohitash@uga.edu

Authors

Charles-Francois V. Latchoumane − *Regenerative Bioscience Center and Edgar L. Rhodes Center for ADS, College of Agriculture and Environmental Sciences, University of Georgia, Athens, Georgia 30602, United States*

Pradeep Chopra − *Complex Carbohydrate Research Center, University of Georgia, Athens, Georgia 30602, United States;* orcid.org/0000-0002-6003-4574

Lifeng Sun − *Department of Chemical Biology and Drug Discovery, Utrecht Institute for Pharmaceutical Sciences, and Bijvoet Center for Biomolecular Research, Utrecht University, Utrecht 3583, The Netherlands*

Aws Ahmed − *Regenerative Bioscience Center, University of Georgia, Athens, Georgia 30602, United States;* orcid.org/0000-0002-7384-1084

Francesco Palmieri − *Department of Chemical Biology and Drug Discovery, Utrecht Institute for Pharmaceutical Sciences, and Bijvoet Center for Biomolecular Research, Utrecht University, Utrecht 3583, The Netherlands*

Hsueh-Fu Wu − *Department of Biochemistry and Molecular Biology, Franklin College of Arts and Sciences and Department of Cellular Biology, Franklin College of Arts and Sciences, University of Georgia, Athens, Georgia 30602, United States*

Rebecca Guerreso − *Regenerative Bioscience Center and Edgar L. Rhodes Center for ADS, College of Agriculture and Environmental Sciences, University of Georgia, Athens, Georgia 30602, United States*

Kristen Thorne − *Complex Carbohydrate Research Center, University of Georgia, Athens, Georgia 30602, United States*

Nadja Zeltner − *Department of Biochemistry and Molecular Biology, Franklin College of Arts and Sciences, Department of Cellular Biology, Franklin College of Arts and Sciences, Center for Molecular Medicine, and Division of Neuroscience, Biomedical and Translational Sciences Institute, University of Georgia, Athens, Georgia 30602, United States*

Complete contact information is available at: https://pubs.acs.org/10.1021/acsami.2c01575

Author Contributions

¶C.-F.V.L. and P.C. contributed equally to this work.

Author Contributions

C.-F.V.L., P.C., G.-J.B., and L.K. designed the research. C.-F.V.L., P.C., L.S., A.A., F.P., R.G., H.-F.W., and K.T. performed the research. C.-F.V.L., P.C., N.Z., G.-J.B., and L.K. analyzed the data. C.-F.V.L., P.C., G.-J.B., and L.K. wrote the manuscript.

Notes

The authors declare no competing financial interest.

■ ACKNOWLEDGMENTS

This work was supported by National Institutes of Health (grants P41GM103390 and HLBI R01HL151617 to G.-J.B. and grant RO1NS099596 to L.K.), partially supported by a Georgia Partners in Regenerative Medicine seed grant from the Regenerative Engineering and Medicine (REM) research center to L.K., and an Alliance for Regenerative Rehabilitation Research and Training (AR^3T) technology development grant to L.K. and C.-F.L.

■ REFERENCES

(1) Bishop, J. R.; Schuksz, M.; Esko, J. D. Heparan Sulphate Proteoglycans Fine-Tune Mammalian Physiology. *Nature* **2007**, *446*, 1030−1037.

(2) Leu, S.-J.; Chen, N.; Chen, C.-C.; Todorović, V.; Bai, T.; Juric, V.; Liu, Y.; Yan, G.; Lam, S. C.-T.; Lau, L. F. Targeted Mutagenesis of the Angiogenic Protein CCN1 (CYR61) Selective Inactivation of Integrin $\alpha 6\beta 1$-Heparan Sulfate Proteoglycan Coreceptor-Mediated Cellular Functions. *J. Biol. Chem.* **2004**, *279*, 44177−44187. Suarez, S. C.; Pieren, M.; Cariolato, L.; Arn, S.; Hoffmann, U.; Bogucki, A.; Manlius, C.; Wood, J.; Ballmer-Hofer, K. A VEGF-A Splice Variant Defective for Heparan Sulfate and Neuropilin-1 Binding shows Attenuated Signaling through VEGFR-2. *Cell. Mol. Life Sci.* **2006**, *63*, 2067−2077.

(3) Yamaguchi, Y. Heparan Sulfate Proteoglycans in the Nervous System: Their Diverse Roles in Neurogenesis, Axon Guidance, and Synaptogenesis. In *Semin. Cell Dev. Biol.*, 2001; Elsevier: Vol. *12*, pp. 99−106.

(4) Yu, C.; Griffiths, L. R.; Haupt, L. M. Exploiting Heparan Sulfate Proteoglycans in Human Neurogenesis—Controlling Lineage Specification and Fate. *Front. Integr. Neurosci.* **2017**, *11*, 28.

(5) Ibrahimi, O. A.; Zhang, F.; Hrstka, S. C.; Mohammadi, M.; Linhardt, R. J. Kinetic model for FGF, FGFR, and proteoglycan signal transduction complex assembly. *Biochemistry* **2004**, *43*, 4724−4730. Walker, A.; Turnbull, J. E.; Gallagher, J. T. Specific heparan sulfate saccharides mediate the activity of basic fibroblast growth factor. *J. Biol. Chem.* **1994**, *269*, 931−935. Asada, M.; Shinomiya, M.; Suzuki, M.; Honda, E.; Sugimoto, R.; Ikekita, M.; Imamura, T. Glycosaminoglycan affinity of the complete fibroblast growth factor family. *Biochim. Biophys. Acta* **2009**, *1790*, 40−48.

(6) Sterner, E.; Meli, L.; Kwon, S. J.; Dordick, J. S.; Linhardt, R. J. FGF-FGFR Signaling Mediated through Glycosaminoglycans in Microtiter Plate and Cell-Based Microarray Platforms. *Biochemistry* **2013**, *52*, 9009−9019. Michalak, A. L.; Trieger, G. W.; Trieger, K. A.; Godula, K. Stem Cell Microarrays for Assessing Growth Factor Signaling in Engineered Glycan Microenvironments. *Adv. Healthcare Mater.* **2022**, *11*, No. e2101232.

(7) Bülow, H. E.; Berry, K. L.; Topper, L. H.; Peles, E.; Hobert, O. Heparan Sulfate Proteoglycan-Dependent Induction of Axon Branching and Axon Misrouting by the Kallmann Syndrome Gene kal-1. *Proc. Natl. Acad. Sci. U. S. A.* **2002**, *99*, 6346−6351. Yi, W.; Clark, P. M.; Mason, D. E.; Keenan, M. C.; Hill, C.; Goddard, W. A.; Peters, E. C.; Driggers, E. M.; Hsieh-Wilson, L. C. Phosphofructokinase 1 Glycosylation Regulates Cell Growth and Metabolism. *Science* **2012**, *337*, 975−980. Díaz-Balzac, C. A.; Lázaro-Peña, M. I.; Tecle, E.; Gomez, N.; Bülow, H. E. Complex Cooperative Functions of Heparan Sulfate Proteoglycans Shape Nervous System Development in Caenorhabditis Elegans. *G3: Genes, Genomes, Genet.* **2014**, *4*, 1859−1870. Saied-Santiago, K.; Townley, R. A.; Attonito, J. D.; Da Cunha, D. S.; Díaz-Balzac, C. A.; Tecle, E.; Bülow, H. E. Coordination of Heparan Sulfate Proteoglycans with Wnt Signaling to Control Cellular Migrations and Positioning in Caenorhabditis Elegans. *Genetics* **2017**, *206*, 1951−1967.

(8) Bülow, H. E.; Hobert, O. Differential Sulfations and Epimerization Define Heparan Sulfate Specificity in Nervous System Development. *Neuron* **2004**, *41*, 723−736. Gama, C. I.; Tully, S. E.; Sotogaku, N.; Clark, P. M.; Rawat, M.; Vaidehi, N.; Goddard, W. A.; Nishi, A.; Hsieh-Wilson, L. C. Sulfation Patterns of Glycosaminoglycans Encode Molecular Recognition and Activity. *Nat. Chem. Biol.* **2006**, *2*, 467−473.

(9) Woodbury, M. E.; Ikezu, T. Fibroblast growth factor-2 signaling in neurogenesis and neurodegeneration. *J. Neuroimmune Pharmacol.* **2014**, *9*, 92−101.

(10) Werner, S.; Unsicker, K.; von Bohlen und Halbach, O. Fibroblast growth factor-2 deficiency causes defects in adult hippocampal neurogenesis, which are not rescued by exogenous fibroblast growth factor-2. *J. Neurosci. Res.* **2011**, *89*, 1605−1617.

(11) Aoyagi, A.; Nishikawa, K.; Saito, H.; Abe, K. Characterization of basic fibroblast growth factor-mediated acceleration of axonal branching in cultured rat hippocampal neurons. *Brain Res.* **1994**, *661*, 117−126.

(12) Chambers, B. J.; Klein, N. W.; Conrad, S. H.; Ruppenthal, G. C.; Sackett, G. P.; Weeks, B. S.; Kleinman, H. K. Reproduction and Sera Embryotoxicity After Immunization of Monkeys with the Laminin Peptides YIGSR, RGD, and IKVAV. *Proc. Natl. Acad. Sci. U. S. A.* **1995**, *92*, 6818−6822. Flanagan, L. A.; Rebaza, L. M.; Derzic, S.; Schwartz, P. H.; Monuki, E. S. Regulation of Human Neural Precursor Cells by Laminin and Integrins. *J. Neurosci. Res.* **2006**, *83*, 845−856.

(13) Li, X.; Liu, X.; Josey, B.; Chou, C. J.; Tan, Y.; Zhang, N.; Wen, X. Short Laminin Peptide for Improved Neural Stem Cell Growth. *Stem Cells Transl. Med.* **2014**, *3*, 662−670.

(14) Varun, D.; Srinivasan, G. R.; Tsai, Y.-H.; Kim, H.-J.; Cutts, J.; Petty, F.; Merkley, R.; Stephanopoulos, N.; Dolezalova, D.; Marsala, M.; Brafman, D. A. A Robust Vitronectin-Derived Peptide for the Scalable Long-Term Expansion and Neuronal Differentiation of Human Pluripotent Stem Cell (hPSC)-Derived Neural Progenitor Cells (hNPCs). *Acta Biomater.* **2017**, *48*, 120−130.

(15) Freeman, R.; Stephanopoulos, N.; Alvarez, Z.; Lewis, J. A.; Sur, S.; Serrano, C. M.; Boekhoven, J.; Lee, S. S.; Stupp, S. I. Instructing Cells with Programmable Peptide DNA Hybrids. *Nat. Commun.* **2017**, *8*, 15982.

(16) Anderson, A. A.; Kendal, C. E.; Garcia-Maya, M.; Kenny, A. V.; Morris-Triggs, S. A.; Wu, T.; Reynolds, R.; Hohenester, E.; Saffell, J. L. A Peptide from the First Fibronectin Domain of NCAM Acts as an Inverse Agonist and Stimulates FGF Receptor Activation, Neurite Outgrowth and Survival. *J. Neurochem.* **2005**, *95*, 570−583.

(17) Williams, E. J.; Williams, G.; Howell, F. V.; Skaper, S. D.; Walsh, F. S.; Doherty, P. Identification of an N-Cadherin Motif that can Interact with the Fibroblast Growth Factor Receptor and is Required for Axonal Growth. *J. Biol. Chem.* **2001**, *276*, 43879−43886.

(18) Chopra, P.; Logun, M. T.; White, E. M.; Lu, W.; Locklin, J.; Karumbaiah, L.; Boons, G.-J. Fully Synthetic Heparan Sulfate-Based Neural Tissue Construct That Maintains the Undifferentiated State of Neural Stem Cells. *ACS Chem. Biol.* **2019**, *14*, 1921−1929.

(19) Goodger, S. J.; Robinson, C. J.; Murphy, K. J.; Gasiunas, N.; Harmer, N. J.; Blundell, T. L.; Pye, D. A.; Gallagher, J. T. Evidence that Heparin Saccharides Promote FGF2 Mitogenesis through Two Distinct Mechanisms. *J. Biol. Chem.* **2008**, *283*, 13001−13008.

(20) Guglieri, S.; Hricovini, M.; Raman, R.; Polito, L.; Torri, G.; Casu, B.; Sasisekharan, R.; Guerrini, M. Minimum FGF2 Binding Structural Requirements of Heparin and Heparan Sulfate Oligosaccharides as Determined by NMR Spectroscopy. *Biochemistry* **2008**, *47*, 13862−13869.

(21) Cederquist, G. Y.; Tchieu, J.; Callahan, S. J.; Ramnarine, K.; Ryan, S.; Zhang, C.; Rittenhouse, C.; Zeltner, N.; Chung, S. Y.; Zhou, T.; Chen, S.; Betel, D.; White, R. M.; Tomishima, M.; Studer, L. A Multiplex Human Pluripotent Stem Cell Platform Defines Molecular and Functional Subclasses of Autism-Related Genes. *Cell Stem Cell* **2020**, *27*, 35−49.e6.

(22) Martin, V. V.; Beierlein, M.; Morgan, J. L.; Rothe, A.; Gee, K. R. Novel Fluo-4 Analogs for Fluorescent Calcium Measurements. *Cell Calcium* **2004**, *36*, 509−514.

(23) Chopra, P.; Joshi, A.; Wu, J.; Lu, W.; Yadavalli, T.; Wolfert, M. A.; Shukla, D.; Zaia, J.; Boons, G.-J. The 3-O-Sulfation of Heparan Sulfate Modulates Protein Binding and Lyase Degradation. *Proc. Natl. Acad. Sci. U. S. A.* **2021**, *118*, No. e2012935118.

(24) Ning, X.; Guo, J.; Wolfert, M. A.; Boons, G.-J. Visualizing Metabolically Labeled Glycoconjugates of Living Cells by Copper-Free and Fast Huisgen Cycloadditions. *Angew. Chem., Int. Ed.* **2008**, *47*, 2253−2255.

(25) Arungundram, S.; Al-Mafraji, K.; Asong, J.; Leach, F. E.; Amster, I. J.; Venot, A.; Turnbull, J. E.; Boons, G.-J. Modular Synthesis of Heparan Sulfate Oligosaccharides for Structure−Activity Relationship Studies. *J. Am. Chem. Soc.* **2009**, *131*, 17394−17405.

(26) Gotoh, N. Control of Stemness by Fibroblast Growth Factor Signaling in Stem Cells and Cancer Stem Cells. *Curr. Stem Cell Res. Ther.* **2009**, *4*, 9−15.

(27) Elkabetz, Y.; Studer, L. Human ESC-Derived Neural Rosettes and Neural Stem Cell Progression. In *Cold Spring Harb. Symp. Quant. Biol.*, 2008; Cold Spring Harbor Laboratory Press: Vol. 73, pp. 377−387. Gabay, L.; Lowell, S.; Rubin, L. L.; Anderson, D. J. Deregulation of Dorsoventral Patterning by FGF Confers Trilineage Differentiation Capacity on CNS Stem Cells In Vitro. *Neuron* **2003**, *40*, 485−499.

(28) Duchesne, L.; Tissot, B.; Rudd, T. R.; Dell, A.; Fernig, D. G. N-Glycosylation of Fibroblast Growth Factor Receptor 1 Regulates Ligand and Heparan Sulfate Co-Receptor Binding. *J. Biol. Chem.* **2006**, *281*, 27178−27189. Li, Y.-C.; Ho, I.-H.; Ku, C.-C.; Zhong, Y.-Q.; Hu, Y.-P.; Chen, Z.-G.; Chen, C.-Y.; Lin, W.-C.; Zulueta, M. M. L.; Hung, S.-C.; Lin, M. G.; Wang, C. C.; Hsiao, C. D. Interactions that Influence the Binding of Synthetic Heparan Sulfate based Disaccharides to Fibroblast Growth Factor-2. *ACS Chem. Biol.* **2014**, *9*, 1712−1717. Zhu, H.; Duchesne, L.; Rudland, P. S.; Fernig, D. G. The Heparan Sulfate Co-receptor and the Concentration of Fibroblast Growth Factor-2 Independently Elicit Different Signalling Patterns from the Fibroblast Growth Factor Receptor. *Cell Commun. Signaling* **2010**, *8*, 14.

(29) Faham, S.; Hileman, R.; Fromm, J.; Linhardt, R.; Rees, D. Heparin Structure and Interactions with Basic Fibroblast Growth Factor. *Science* **1996**, *271*, 1116−1120.

(30) Schlessinger, J.; Plotnikov, A. N.; Ibrahimi, O. A.; Eliseenkova, A. V.; Yeh, B. K.; Yayon, A.; Linhardt, R. J.; Mohammadi, M. Crystal Structure of a Ternary FGF-FGFR-Heparin Complex Reveals a Dual Role for Heparin in FGFR Binding and Dimerization. *Mol. Cell* **2000**, *6*, 743−750.

(31) Capicciotti, C. J.; Zong, C.; Sheikh, M. O.; Sun, T.; Wells, L.; Boons, G.-J. Cell-Surface Glyco-Engineering by Exogenous Enzymatic

https://doi.org/10.1021/acsami.2c01575
ACS Appl. Mater. Interfaces 2022, 14, 28476−28488

Transfer using a Bifunctional CMP-Neu5Ac Derivative. *J. Am. Chem. Soc.* **2017**, *139*, 13342−13348.
(32) Shipp, E. L.; Hsieh-Wilson, L. C. Profiling the Sulfation Specificities of Glycosaminoglycan Interactions with Growth Factors and Chemotactic Proteins using Microarrays. *Chem. Biol.* **2007**, *14*, 195−208.
(33) Guillonneau, X.; Tassin, J.; Berrou, E.; Bryckaert, M.; Courtois, Y.; Mascarelli, F. In Vitro Changes in Plasma Membrane Heparan Sulfate Proteoglycans and in Perlecan Expression Participate in the Regulation of Fibroblast Growth Factor 2 Mitogenic Activity. *J. Cell. Physiol.* **1996**, *166*, 170−187.
(34) Mossahebi-Mohammadi, M.; Quan, M.; Zhang, J. S.; Li, X. FGF Signaling Pathway: A Key Regulator of Stem Cell Pluripotency. *Front. Cell Dev. Biol.* **2020**, *8*, 79.
(35) Ditlevsen, D. K.; Berezin, V.; Bock, E. Signalling Pathways Underlying Neural Cell Adhesion Molecule-Mediated Survival of Dopaminergic Neurons. *Eur. J. Neurosci.* **2007**, *25*, 1678−1684. Ruardij, T.; Goedbloed, M.; Rutten, W. Long-Term Adhesion and Survival of Dissociated Cortical Neurons on Miniaturised Chemical Patterns. *Med. Biol. Eng. Comput.* **2003**, *41*, 227−232.
(36) Seidlits, S. K.; Liang, J.; Bierman, R. D.; Sohrabi, A.; Karam, J.; Holley, S. M.; Cepeda, C.; Walthers, C. M. Peptide-Modified, Hyaluronic Acid-based Hydrogels as a 3D Culture Platform for Neural Stem/Progenitor Cell Engineering. *J. Biomed. Mater. Res. A* **2019**, *107*, 704−718.

https://doi.org/10.1021/acsami.2c01575
ACS Appl. Mater. Interfaces 2022, 14, 28476−28488